Supporting Information

Anomalous redshift emission in Pt(II) vs Ir(III) complexes with identical ligands and the application of these complexes in high-efficiency OLED

Wenping Liu[a], Shipan Xu[a], Xuyang Du[a], An Yan[a], Shengli Li[a], Xiaolong Yang[a,*] Jun Xi[b], Yousong Ding[c], Guijiang Zhou[a,*] and Yuanhui Sun[a,*]

[a] *School of Chemistry, Xi'an Key Laboratory of Sustainable Energy Material Chemistry, Engineering Research Center of Energy Storage Materials and Devices, Ministry of Education, Xi'an Jiaotong University, Xi'an 710049, China*

[b] *School of Electronic Science and Engineering, Xi'an Jiaotong University, Xi'an 710049, China*

[c] *Department of Chemistry, Southern University of Science and Technology, Shenzhen, 518055, China*

[*] Corresponding authors

E-mail addresses: zhougj@xjtu.edu.cn (G. Zhou), sunyuanhui@xjtu.edu.cn (Y. Sun), xiaolongyang@xjtu.edu.cn (X. Yang)

General experimental information

Commercially available starting materials were used directly without further purification. ^{1}H NMR and ^{13}C NMR spectra were measured in $CDCl_3$ on a Bruker Avance 400 MHz spectrometer. Chemical shifts were referenced to the solvent residual peak at δ 7.26 ppm for ^{1}H and 77.0 ppm for ^{13}C, respectively. Mass spectra (MS) measurements were performed on WATERS I-Class VION IMS QTof. The thermal stability of these complexes ware tested on a NETZSCH STA 409C instrument under N_2 at a heating rate of 20 K min^{-1}. UV-vis absorption spectra were measured on a Lambda 950 spectrophotometer in dichloromethane at room temperature. Photoluminescent spectra and lifetimes of these complexes were measured on an Edinburgh Instruments Ltd (FLs920) fluorescence spectrophotometer. The solution PLQYs were determined in degassed CH_2Cl_2 solutions at room temperature against *fac*-$(piq)_2Ir(acac)$ standard (PLQY = 0.2). Calibrated with ferrocene/ferrocenium (Fc/Fc^+) couple, cyclic voltammetry investigations were conducted on a Princeton Applied Research (PARSTAT 2273, Advanced Electrochemical System) equipment in CH_3CN solutions containing *n*-Bu_4NPF_6 (0.1 M) as the supporting electrolyte under a N_2 atmosphere. The scan rate was 100 mV s^{-1}. The HOMO and LUMO energy levels were calculated using the oxidation potential (E_{ox}) and reduction potential (E_{red}) according to the equations $E_{HOMO} = -(E_{ox} + 4.8)$ eV and $E_{LUMO} = -(E_{red} + 4.8)$ eV.

X-ray diffraction investigation. The single crystals of Pt(II) complexes MBTQ-Ir and MBTQ-Pt were prepared by slowly diffusing their CH_2Cl_2 solutions into methanol at room temperature. The X-ray diffraction data were collected using a Bruker D8

Venture diffractometer on a rotating anode (Mo-K radiation, 0.71073 Å) at 150 K. The structure was solved and refined by the direct method using SHELXT and refined with Olex2[1-3].

Theoretical computation. Theoretical calculations were performed for all these Pt(II) complexes based on density functional theory (DFT) and time dependent-DFT (TD-DFT) calculations.[4, 5] Non-metal atoms of C, H, N, O, and S were calculated based on B3LYP/6-31G(d, p). The Pt and Ir atoms were calculated based on B3LYP/LanL2DZ. The excitation behaviors of the complexes were calculated by TD-DFT method based on optimized geometries at the ground states. All calculations were carried out by using the Gaussian 16 program.[6]

OLED fabrication and measurements. All the organic layers were successively deposited by means of vacuum deposition onto the ITO-coated glass substrates, which were previously etched, patterned, and washed with detergent, deionized water, acetone, and ethanol in turn. For the doped layer, the dopant and host materials were co-evaporated and the doping concentrations was controlled by deposition rates. The electroluminescence (EL) spectra and CIE coordinates of the devices were measured by a spectrometer (PR655) and the current-voltage-luminescence characteristics were analyzed using Keithley 2400 source meter with PR655.

General procedure for synthesizing these Pt(II) and Ir(III) complexes.

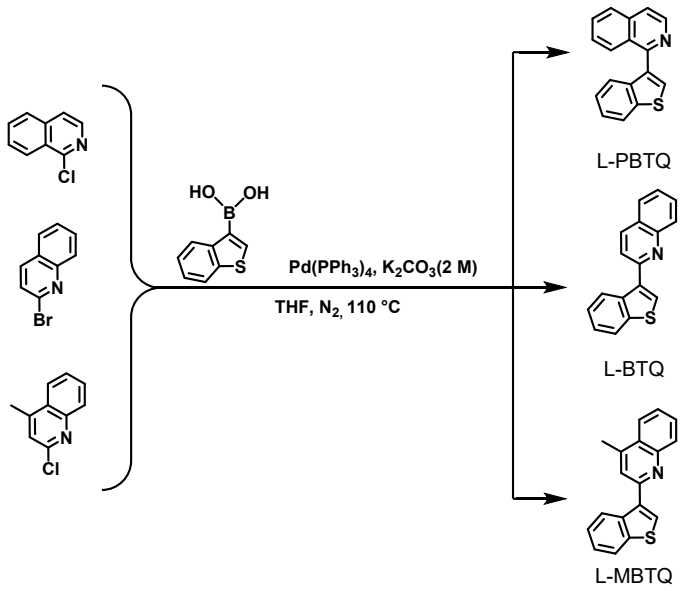

Scheme S1. Synthesis route of ligand**.**

Ligand L-PBTQ: Under a N_2 atmosphere, benzo[b]thiophen-3-ylboronic acid (1200 mg, 7.33 mmol), 2-chloroisoquinoline (1440 mg, 8.07 mmol), and $Pd(PPh_3)_4$ (420 mg, 0.36 mmol) were added to a mixture of THF (20 mL) and 2 M K_2CO_3 aqueous solution (20 mL). The reaction mixture was stirred at 110 °C under reflux for 12 h. After cooling to room temperature, the mixture was poured into water (50 mL) and extracted with dichloromethane several times. The combined organic layers were dried over anhydrous $MgSO_4$ and concentrated under reduced pressure. The crude product was purified by thin-layer chromatography using homemade silica gel to afford the desired product as a solid (1.30 g, 70%). ^{1}H NMR (400 MHz, $CDCl_3$) δ 8.68 (d, J = 5.6 Hz, 1H), 8.04 (d, J = 8.5 Hz, 1H), 7.97 (d, J = 8.0 Hz, 1H), 7.92 (d, J = 8.3 Hz, 1H), 7.74 – 7.68 (m, 4H), 7.54 – 7.49 (m, 1H), 7.43 – 7.32 (m, 2H).

Ligand L-BTQ: Under a N_2 atmosphere, benzo[b]thiophen-3-ylboronic acid (1000 mg, 5.62 mmol), 2-Bromoquinoline (900 mg, 4.33 mmol), and $Pd(PPh_3)_4$ (250 mg, 0.21

mmol) were added to a mixture of THF (20 mL) and 2 M K_2CO_3 aqueous solution (20 mL). The reaction mixture was stirred at 110 °C under reflux for 12 h. After cooling to room temperature, the mixture was poured into water (50 mL) and extracted with dichloromethane several times. The combined organic layers were dried over anhydrous $MgSO_4$ and concentrated under reduced pressure. The crude product was purified by thin-layer chromatography using homemade silica gel to afford the desired product as a solid (1300 mg, 96%). ^{1}H NMR (400 MHz, $CDCl_3$) δ 8.83 (d, *J* = 8.3 Hz, 1H), 8.23 (d, *J* = 8.5 Hz, 2H), 7.98 – 7.92 (m, 2H), 7.84 (d, *J* = 16.0 Hz, 2H), 7.75 (d, *J* = 7.0 Hz, 1H), 7.59 – 7.48 (m, 2H), 7.44 (t, *J* = 7.5 Hz, 1H).

Ligand L-BTQ: Under a N_2 atmosphere, benzo[b]thiophen-3-ylboronic acid (1.20 g, 6.75 mmol), 2-chlorolepidine (1000 mg, 5.63 mmol), and $Pd(PPh_3)_4$ (320 g, 0.28 mmol) were added to a mixture of THF (20 mL) and 2 M K_2CO_3 aqueous solution (20 mL). The reaction mixture was stirred at 110 °C under reflux for 12 h. After cooling to room temperature, the mixture was poured into water (50 mL) and extracted with dichloromethane several times. The combined organic layers were dried over anhydrous $MgSO_4$ and concentrated under reduced pressure. The crude product was purified by thin-layer chromatography using homemade silica gel to afford the desired product as a solid (1420 mg, 92%). ^{1}H NMR (400 MHz, $CDCl_3$) δ 8.79 (d, *J* = 7.9 Hz, 1H), 8.23 (d, *J* = 8.4 Hz, 1H), 8.03 (d, *J* = 8.3 Hz, 1H), 7.94 (d, *J* = 10.3 Hz, 2H), 7.75 (t, *J* = 7.6 Hz, 1H), 7.68 (s, 1H), 7.58 (t, *J* = 8.3 Hz, 1H), 7.52 – 7.46 (m, 1H), 7.42 (t, *J* = 7.5 Hz, 1H), 2.79 (s, 3H).

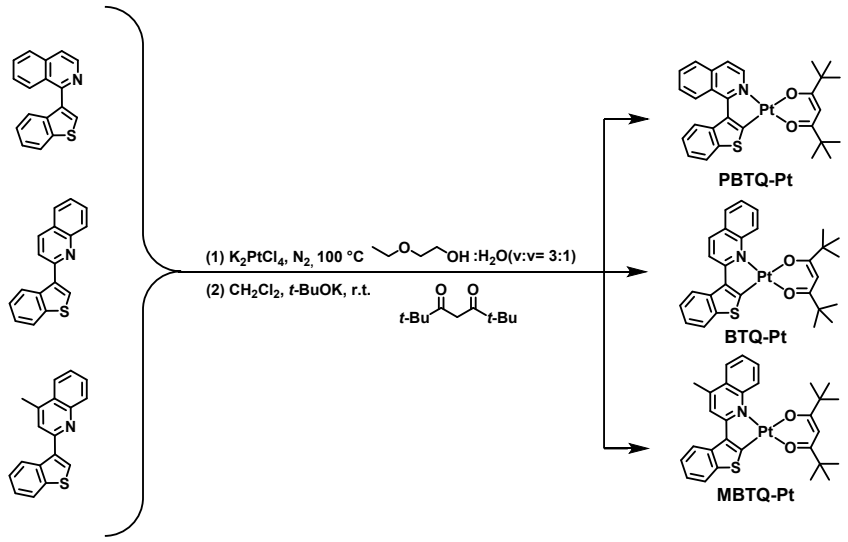

Scheme S2. Synthesis route of Pt(II) complexes**.**

PBTQ-Pt: Under a N_2 atmosphere, the mixture solution of 2-Ethoxyethanol and H_2O (3:1, *v/v*) (30 mL), ligand L-PBTQ (100 mg, 0.38 mmol), and K_2PtCl_4 (16 mg, 0.38 mmol) was heated to 100 °C and stirred for ca. 12 h. After being cooled to room temperature, the mixture was extracted with CH_2Cl_2 several times. The collected organic layers were dried over anhydrous Na_2SO_4. After the removal of the solvent, the residual dimer was readily dissolved in CH_2Cl_2. After half an hour of activation by adding *t*-BuOK (129 mg, 1.15 mmol) and 2,2,6,6-tetramethyl-3,5-heptanedione (212 mg, 1.15 mmol), dimer dissolved in CH_2Cl_2 (20 mL) were added, the mixture was stirred at room temperature for ca. 12 h under a N_2 atmosphere. The reaction was quenched with water upon completion and extracted three times with dichloromethane. The combined organic phases were dried over anhydrous sodium sulfate and concentrated under reduced pressure. The residual was purified on self-made silica TLC (TLC plates were self-prepared using fine silica gel and an aqueous solution of carboxymethyl cellulose sodium (1.25 g/L)). The developing agent was petroleum

ether/dichloromethane (4:1, v/v). The target band was scraped off and eluted with dichloromethane to give the desired Pt(II) complexes. (Total yield, 59%). ^{1}H NMR(400 MHZ, $CDCl_3$):δ 8.73 (dd, *J* = 7.5, 3.9 Hz, 2H), 8.08 (d, *J* = 8.1 Hz, 1H), 7.87 – 7.81 (m, 2H), 7.77 – 7.72 (m, 1H), 7.65 – 7.58 (m, 1H), 7.38 (d, *J* = 6.5 Hz, 1H), 7.31 – 7.27 (m, 1H), 7.19 (t, *J* = 8.1 Hz, 1H), 5.90 (s, 1H), 1.32 (d, *J* = 3.7 Hz, 18H); ^{13}C NMR(101 MHz, $CDCl_3$) δ 195.12, 194.05, 167.10, 161.10, 142.02, 138.81, 138.26, 137.99, 137.84, 131.72, 128.79, 126.43, 126.03, 123.99, 123.88, 123.08, 121.55, 121.41, 116.66, 93.55, 41.55, 41.51, 28.51, 28.40. ESI-MS (*m/z*) : $[M + Na]^+$,661.1458; found, 661.1498.

BTQ-Pt: Under a N_2 atmosphere, the mixture solution of 2-Ethoxyethanol and H_2O (3:1, *v/v*) (30 mL), ligand L-BTQ (100 mg, 0.38 mmol,) and K_2PtCl_4 (100 mg, 0.38 mmol) was heated to 100 °C and stirred for ca. 12 h. After being cooled to room temperature, the mixture was extracted with CH_2Cl_2 several times. The collected organic layers were dried over anhydrous Na_2SO_4. After the removal of the solvent, the residual dimer was readily dissolved in CH_2Cl_2. After half an hour of activation by adding *t*-BuOK (129 mg, 1.15 mmol) and 2,2,6,6-tetramethyl-3,5-heptanedione (212 mg, 1.15 mmol), dimer dissolved in CH_2Cl_2 (20 mL) were added, the mixture was stirred at room temperature for ca. 12 h under a N_2 atmosphere. The subsequent processing procedure is the same as described above, obtaining the BTQ-Pt complex. (Total Yield, 25%). ^{1}H NMR(400 MHZ, $CDCl_3$):δ 9.66 (d, *J* = 8.9 Hz, 1H), 8.26 (d, *J* = 8.6 Hz, 1H), 8.08 (dd, *J* = 21.2, 8.4 Hz, 2H), 7.87 (d, *J* = 8.6 Hz, 1H), 7.79 – 7.68 (m, 2H), 7.50 (t, *J* = 7.5 Hz, 1H), 7.37 (t, *J* = 7.0 Hz, 1H), 7.23 (t, *J* = 7.0 Hz, 1H), 5.99 (s,

1H), 1.34 (d, *J* = 6.8 Hz, 18H). ^{13}C NMR (101 MHz, $CDCl_3$) δ 195.33, 193.84, 166.60, 159.70, 150.30, 141.35, 139.73, 138.24, 137.21, 131.12, 127.72, 126.15, 125.45, 125.17, 124.52, 123.17, 121.93, 118.87, 116.85, 92.94, 42.30, 41.45, 28.55. ESI-MS (*m/z*) : $[M + Na]^+$, 661.1458; found, 661.1516.

MBTQ-Pt: Under a N_2 atmosphere, the mixture solution of 2-Ethoxyethanol and H_2O (3:1, *v/v*) (30 mL), ligand L-MBTQ (150 mg, 0.55 mmol,) and K_2PtCl_4 (228 mg, 0.55 mmol) was heated to 100 °C and stirred for ca. 12 h. After being cooled to room temperature, the mixture was extracted with CH_2Cl_2 several times. The collected organic layers were dried over anhydrous Na_2SO_4. After the removal of the solvent, the residual dimer was readily dissolved in CH_2Cl_2. After half an hour of activation by adding *t*-BuOK (185 mg, 1.65 mmol) and 2,2,6,6-tetramethyl-3,5-heptanedione (304 mg, 1.65 mmol), dimer dissolved in CH_2Cl_2 (20 mL) were added, the mixture was stirred at room temperature for ca. 12 h under a N_2 atmosphere. The subsequent processing procedure is the same as described above, obtaining the MBTQ-Pt complex. (Total Yield, 16%). ^{1}H NMR(400 MHZ, $CDCl_3$) : δ 9.63 (d, *J* = 8.9 Hz, 1H), 8.12 (d, *J* = 8.1 Hz, 1H), 7.92 – 7.85 (m, 3H), 7.69 (ddd, *J* = 8.7, 6.9, 1.7 Hz, 1H), 7.51 (t, *J* = 7.6 Hz, 1H), 7.37 (t, *J* = 7.8 Hz, 1H), 7.22 (t, *J* = 7.0 Hz, 1H), 5.97 (s, 1H), 2.85 (s, 3H), 1.34 (d, *J* = 7.9 Hz, 18H). ^{13}C NMR (101 MHz, $CDCl_3$) δ 195.20, 193.74, 165.86, 159.13, 149.69, 148.09, 141.35, 138.33, 137.22, 130.70, 126.04, 125.87, 124.90, 124.38, 123.73, 123.10, 121.80, 118.88, 117.77, 92.86, 42.27, 41.43, 28.54, 19.62. ESI-MS (*m/z*) : $[M + Na]^+$, 675.1615; found, 675.1621.

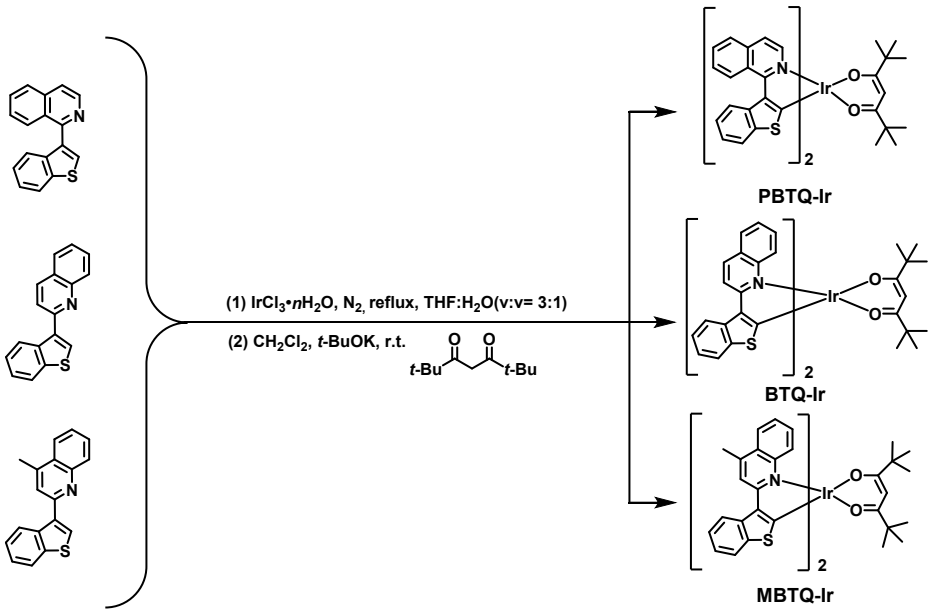

Scheme S3. Synthesis route of Ir(III) complexes**.**

PBTQ-Ir: Under a N_2 atmosphere, the mixture solution of THF and H_2O (3:1, *v/v*) (30 mL), ligand L-PBTQ (150 mg, 0.58 mmol), and $IrCl_3 \cdot nH_2O$ (91 mg, 0.29 mmol) were placed in a sealed reaction tube. The sealed tube was heated to 110°C using magnetic stirrer, maintained at this temperature with stirring for 12 h. After being cooled to room temperature, the mixture was extracted with CH_2Cl_2 several times. The collected organic layers were dried over anhydrous Na_2SO_4. After the removal of the solvent, the residual was readily dissolved in CH_2Cl_2. After half an hour of activation by adding *t*-BuOK (96 mg, 0.86 mmol) and 2,2,6,6-tetramethyl-3,5-heptanedione (159 mg, 0.86 mmol), residues dissolved in CH_2Cl_2 (20 mL) were added, the mixture was stirred at room temperature for ca. 12 h under a N_2 atmosphere. The subsequent processing procedure is the same as described above, obtaining the PBTQ-Ir complex. (Total Yield, 40%). ^{1}H NMR(400 MHZ, $CDCl_3$):δ (ppm) δ 8.83 (d, J = 8.4 Hz, 2H), 8.13 (dd, J = 7.3, 5.1 Hz, 4H), 7.90 (d, J = 8.2 Hz, 2H), 7.73 (t, J = 6.8 Hz, 2H), 7.65 (t, J = 6.9 Hz, 2H), 7.54 (d, J = 7.8 Hz, 2H), 7.37 (d, J = 6.4 Hz, 2H), 7.24 – 7.19 (m, 2H), 7.01

(t, *J* = 8.1 Hz, 2H), 5.51 (s, 1H), 0.84 (s, 18H). ^{13}C NMR (101 MHZ, $CDCl_3$):δ 194.93, 167.85, 167.28, 143.95, 140.65, 138.52, 138.02, 137.65, 131.23, 128.75, 126.14, 125.35, 124.09, 123.42, 122.22, 121.06, 120.34, 116.23, 90.18, 41.12, 28.02. ESI-MS (*m/z*) : $[M + Na]^+$, 919.1974; found, 919.2003.

BTQ-Ir: Under a N_2 atmosphere, the mixture solution of THF and H_2O (3:1, *v/v*) (30 mL), ligand L-BTQ (150 mg, 0.58 mmol), and $IrCl_3 \cdot nH_2O$ (91 mg, 0.29 mmol) were placed in a sealed reaction tube. The sealed tube was heated to 110°C using magnetic stirrer, maintained at this temperature with stirring for 12 h. After being cooled to room temperature, the mixture was extracted with CH_2Cl_2 several times. The collected organic layers were dried over anhydrous Na_2SO_4. After the removal of the solvent, the residual was readily dissolved in CH_2Cl_2. After half an hour of activation by adding *t*-BuOK (96 mg, 0.86 mmol) and 2,2,6,6-tetramethyl-3,5-heptanedione (159 mg, 0.86 mmol), residues dissolved in CH_2Cl_2 (20 mL) were added, the mixture was stirred at room temperature for ca. 12 h under a N_2 atmosphere. The subsequent processing procedure is the same as described above, obtaining the BTQ-Ir complex. (Total Yield, 14%). ^{1}H NMR(400 MHZ, $CDCl_3$):δ 8.33 (dd, *J* = 8.7, 3.1 Hz, 4H), 8.23 (dd, *J* = 11.9, 8.2 Hz, 4H), 7.75 (dd, *J* = 7.9, 1.7 Hz, 2H), 7.53 (d, *J* = 7.2 Hz, 2H), 7.44 – 7.40 (m, 2H), 7.37 – 7.32 (m, 4H), 7.09 – 7.05 (m, 2H), 5.09 (s, 1H), 0.67 (s, 18H). ^{13}C NMR δ 8.33 (dd, *J* = 8.7, 3.1 Hz, 4H), 8.23 (dd, *J* = 11.9, 8.2 Hz, 4H), 7.75 (dd, *J* = 7.9, 1.7 Hz, 2H), 7.53 (d, *J* = 7.2 Hz, 2H), 7.44 – 7.40 (m, 2H), 7.37 – 7.32 (m, 4H), 7.09 – 7.05 (m, 2H), 5.09 (s, 1H), 0.67 (s, 18H). ESI-MS (*m/z*) : $[M + Na]^+$, 919.1974; found, 919.2015.

MBTQ-Ir: Under a N_2 atmosphere, the mixture solution of THF and H_2O (3:1, *v/v*) (30 mL), ligand L-MBTQ (150 mg, 0.55 mmol), and $IrCl_3 \cdot nH_2O$ (88 mg, 0.28 mmol) were placed in a sealed reaction tube. The sealed tube was heated to 110°C using magnetic stirrer, maintained at this temperature with stirring for 12 h. After being cooled to room temperature, the mixture was extracted with CH_2Cl_2 several times. The collected organic layers were dried over anhydrous Na_2SO_4. After the removal of the solvent, the residual was readily dissolved in CH_2Cl_2. After half an hour of activation by adding *t*-BuOK (93 mg, 0.83 mmol) and 2,2,6,6-tetramethyl-3,5-heptanedione (152 mg, 0.83 mmol), residues dissolved in CH_2Cl_2 (20 mL) were added, the mixture was stirred at room temperature for ca. 12 h under a N_2 atmosphere. The subsequent processing procedure is the same as described above, obtaining the MBTQ-Ir complex. (Total Yield, 19%). ^{1}H NMR(400 MHZ, $CDCl_3$):δ 8.35 (d, *J* = 7.6 Hz, 2H), 8.26 (d, *J* = 8.3 Hz, 2H), 8.20 (s, 2H), 7.90 (d, *J* = 6.6 Hz, 2H), 7.52 (d, *J* = 7.9 Hz, 2H), 7.46 – 7.41 (m, 2H), 7.36 – 7.30 (m, 4H), 7.05 (t, *J* = 7.9 Hz, 2H), 5.08 (s, 1H), 2.98 (s, 6H), 0.66 (s, 18H). ^{13}C NMR (101 MHz, $CDCl_3$) δ 194.79, 166.57, 165.42, 149.67, 146.96, 144.39, 139.17, 138.21, 130.27, 125.87, 125.33, 124.52, 123.94, 123.51, 122.40, 120.64, 118.41, 117.79, 89.97, 40.61, 27.71, 19.48. ESI-MS (*m/z*) : $[M + Na]^+$, 947.2287; found, 947.2272.

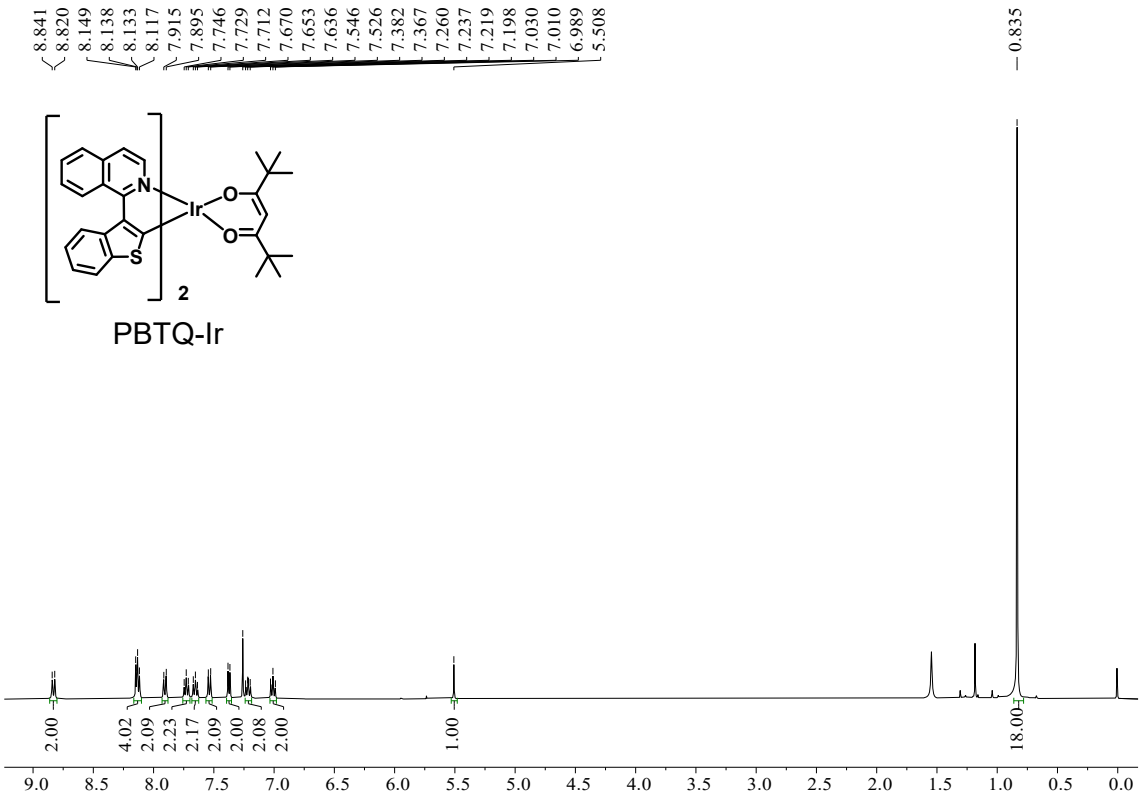
8.841
8.820
8.149
8.138
8.133
8.117
7.915
7.895
7.746
7.729
7.712
7.670
7.653
7.636
7.546
7.526
7.382
7.367
7.260
7.237
7.219
7.198
7.030
7.010
6.989
5.508
0.835
N
Ir
O
O
S
2
PBTQ-Ir
2.00
4.02
2.09
2.23
2.17
2.09
2.00
2.08
2.00
1.00
18.00
9.0
8.5
8.0
7.5
7.0
6.5
6.0
5.5
5.0
4.5
4.0
3.5
3.0
2.5
2.0
1.5
1.0
0.5
0.0

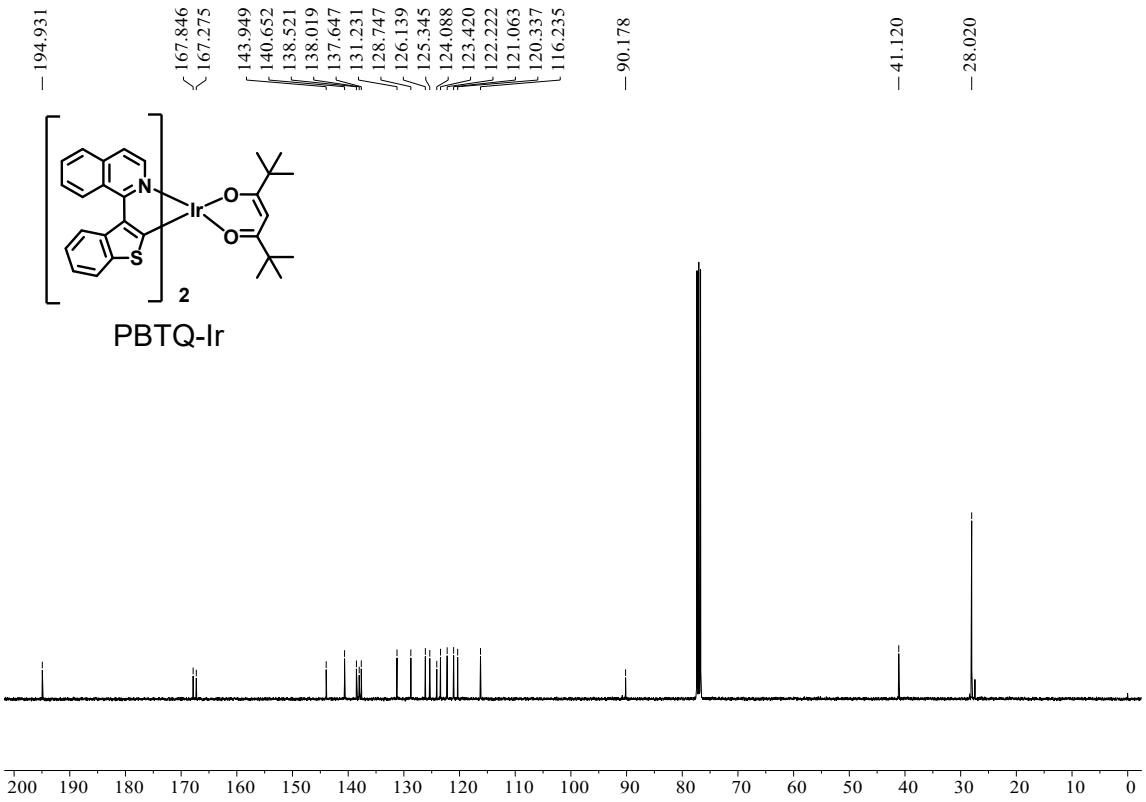
194.931
167.846
167.275
143.949
140.652
138.521
138.019
137.647
131.231
128.747
126.139
125.345
124.088
123.420
122.222
121.063
120.337
116.235
90.178
41.120
28.020
N
Ir
O
O
S
2
PBTQ-Ir
200
190
180
170
160
150
140
130
120
110
100
90
80
70
60
50
40
30
20
10
0

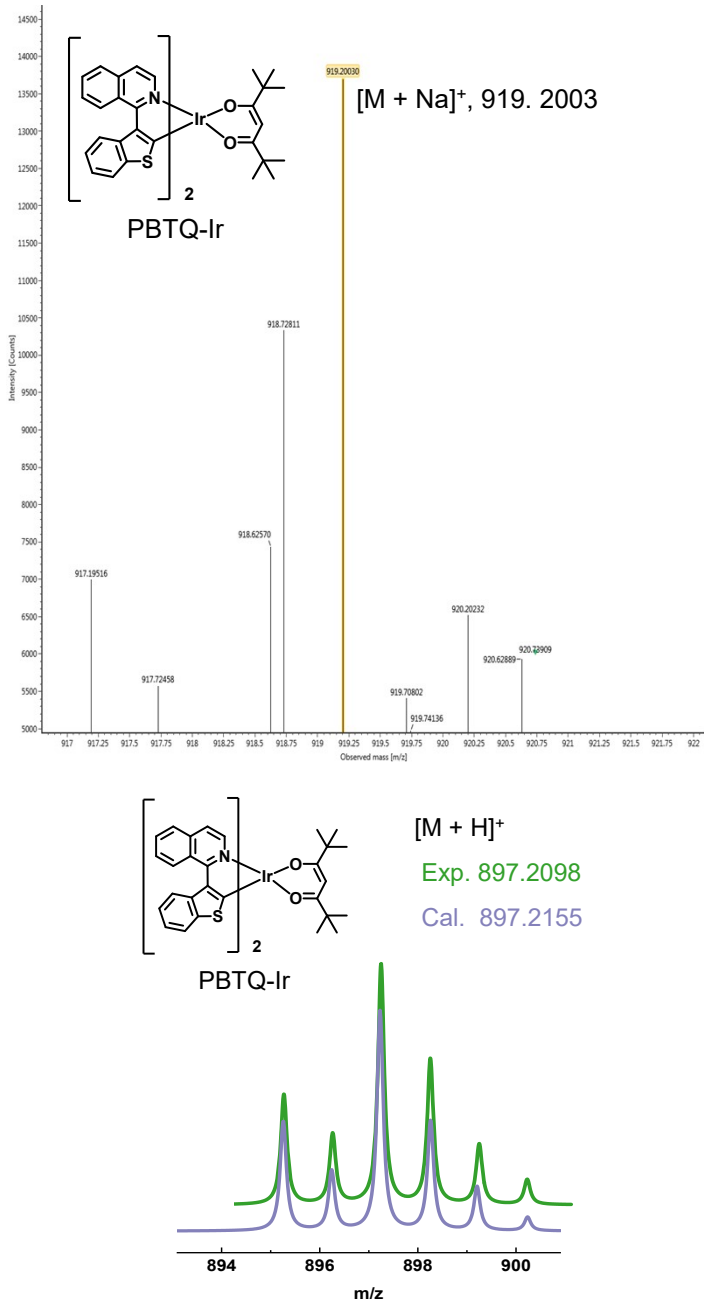

Figure S1. The ^{1}H, ^{13}C, HRMS and the measured (green trace) and simulated (purple trace) isotopic patterns of **PBTQ-Ir**.

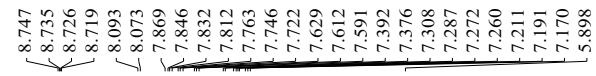

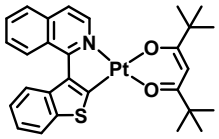

PBTQ-Pt

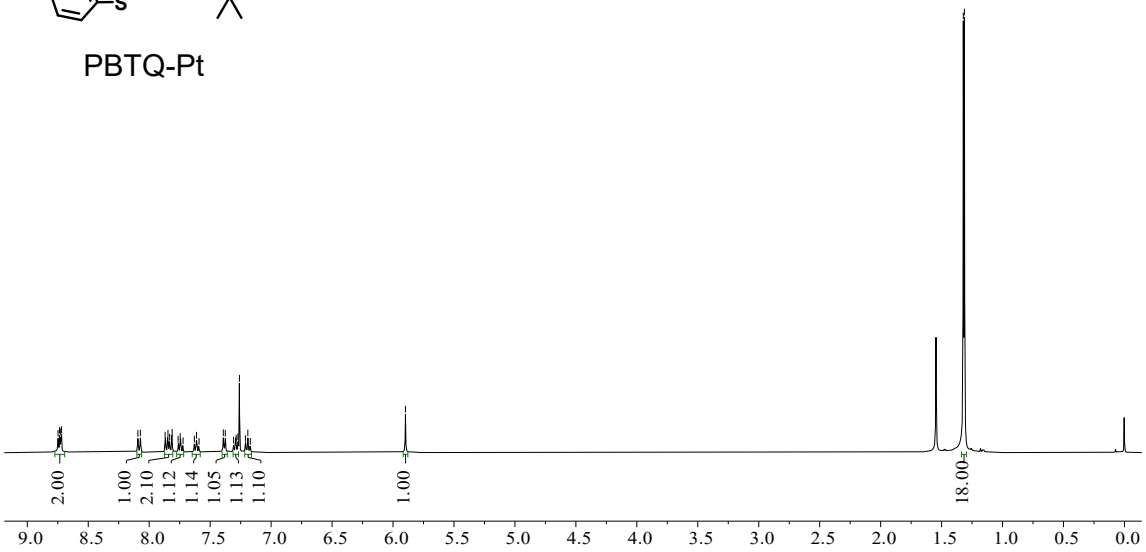

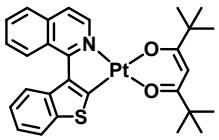

PBTQ-Pt

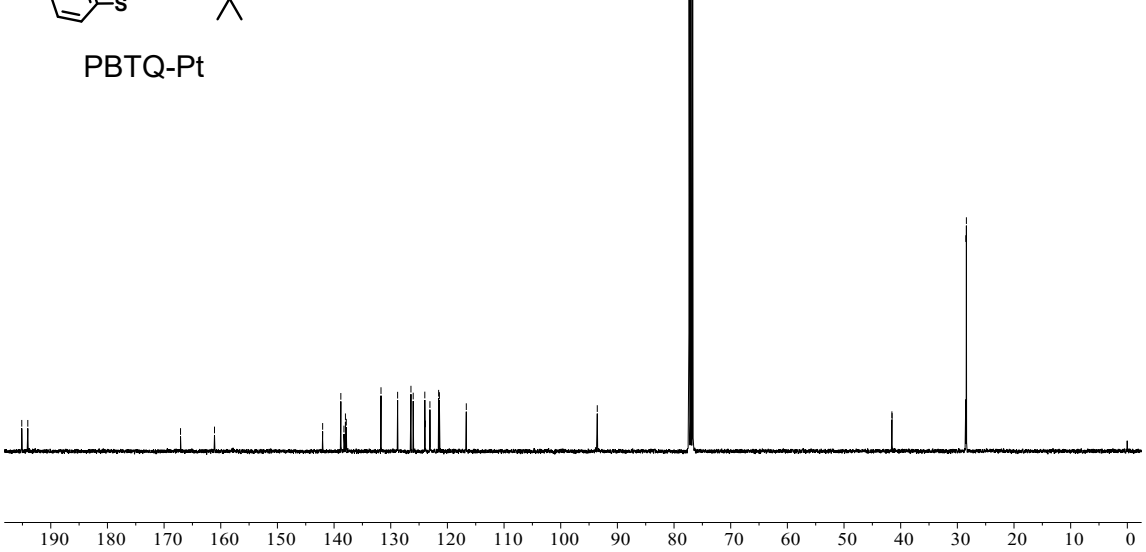

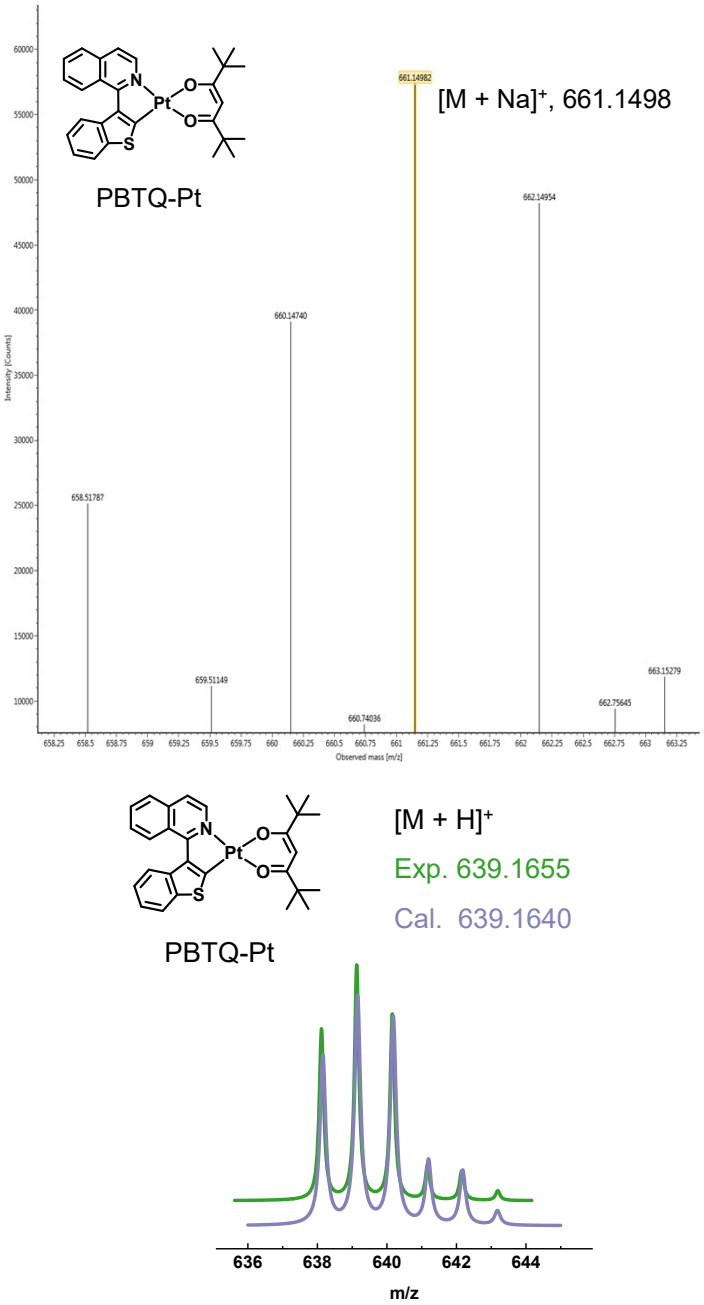

Figure S2. The ^{1}H, ^{13}C, HRMS and the measured (green trace) and simulated (purple trace) isotopic patterns of **PBTQ-Pt**.

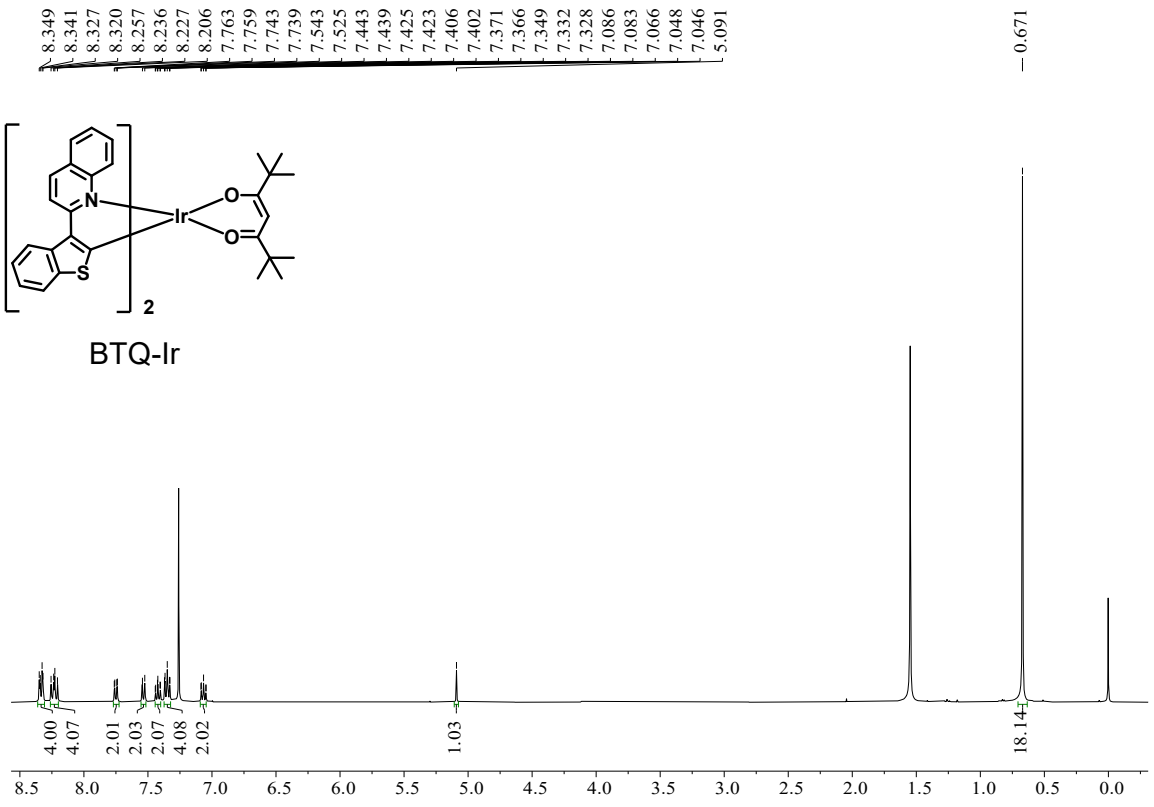
8.349
8.341
8.327
8.320
8.257
8.236
8.227
8.206
7.763
7.759
7.743
7.739
7.543
7.525
7.443
7.439
7.425
7.423
7.406
7.402
7.371
7.366
7.349
7.332
7.328
7.086
7.083
7.066
7.048
7.046
5.091
0.671
N
Ir
O
O
S
2
BTQ-Ir
4.00
4.07
2.01
2.03
2.07
4.08
2.02
1.03
18.14
8.5
8.0
7.5
7.0
6.5
6.0
5.5
5.0
4.5
4.0
3.5
3.0
2.5
2.0
1.5
1.0
0.5
0.0

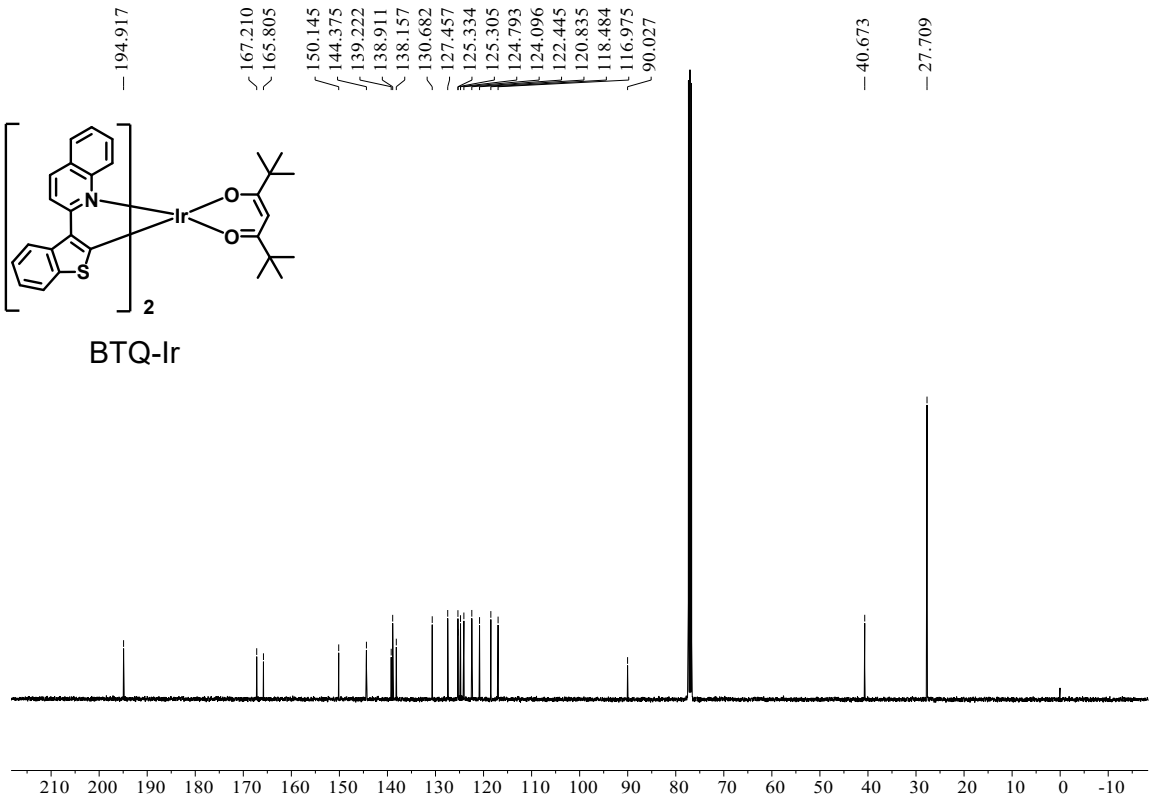
194.917
167.210
165.805
150.145
144.375
139.222
138.911
138.157
130.682
127.457
125.334
125.305
124.793
124.096
122.445
120.835
118.484
116.975
90.027
40.673
27.709
N
Ir
O
O
S
2
BTQ-Ir
210
200
190
180
170
160
150
140
130
120
110
100
90
80
70
60
50
40
30
20
10
0
-10

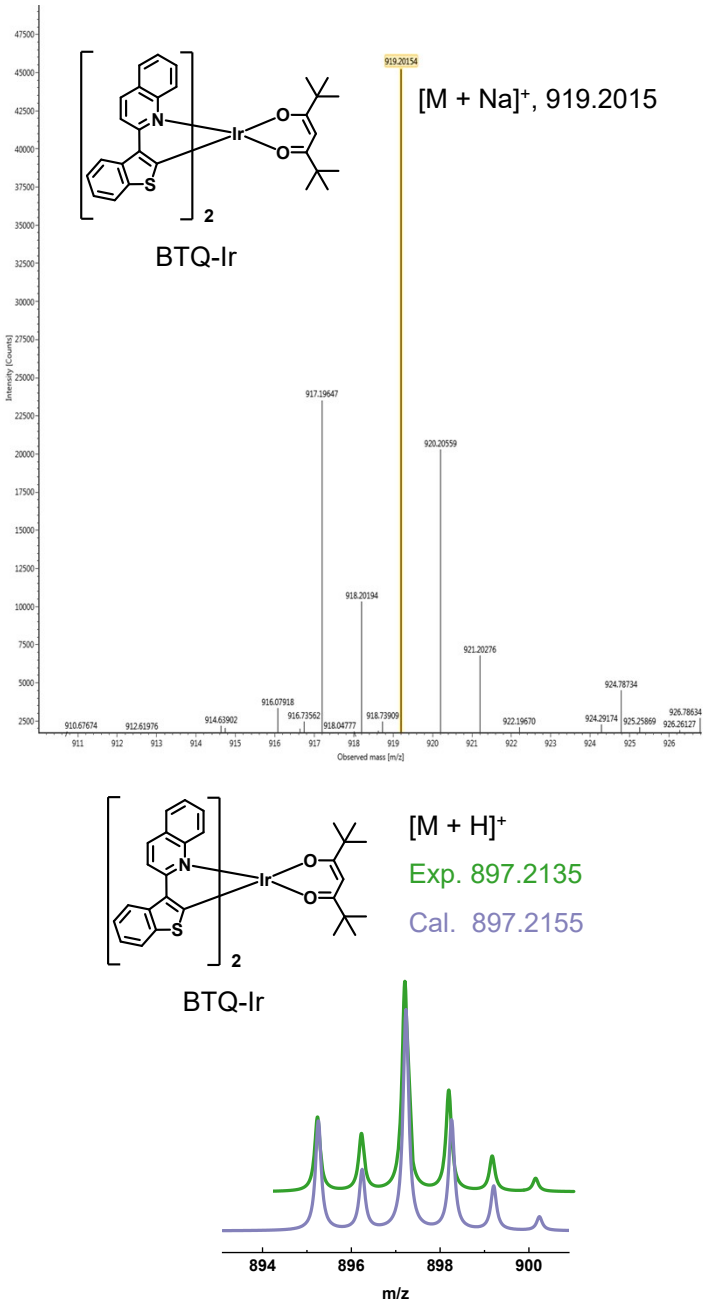

Figure S3. The ^{1}H, ^{13}C, HRMS and the measured (green trace) and simulated (purple trace) isotopic patterns of **BTQ-Ir**.

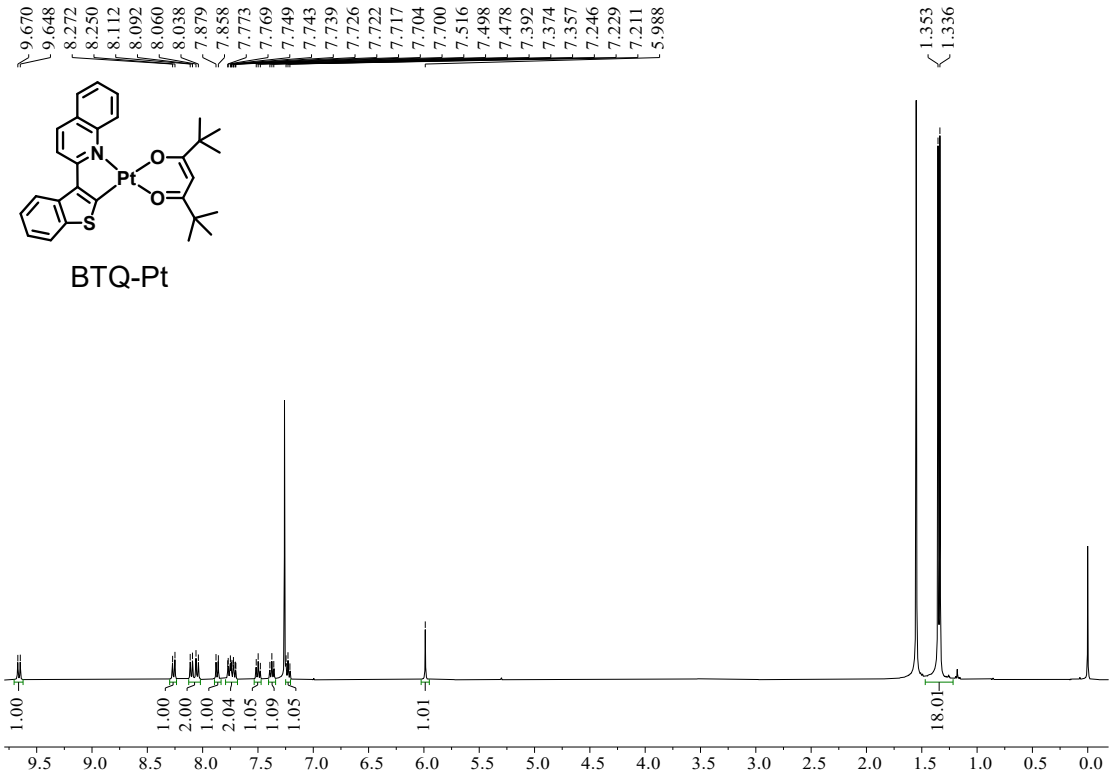
9.670
9.648
8.272
8.250
8.112
8.092
8.060
8.038
7.879
7.858
7.773
7.769
7.749
7.743
7.739
7.726
7.722
7.717
7.704
7.700
7.516
7.498
7.478
7.392
7.374
7.357
7.246
7.229
7.211
5.988
1.353
1.336
N
Pt
O
O
S
BTQ-Pt
1.00
1.00
2.00
1.00
2.04
1.05
1.09
1.05
1.01
18.01
9.5 9.0 8.5 8.0 7.5 7.0 6.5 6.0 5.5 5.0 4.5 4.0 3.5 3.0 2.5 2.0 1.5 1.0 0.5 0.0

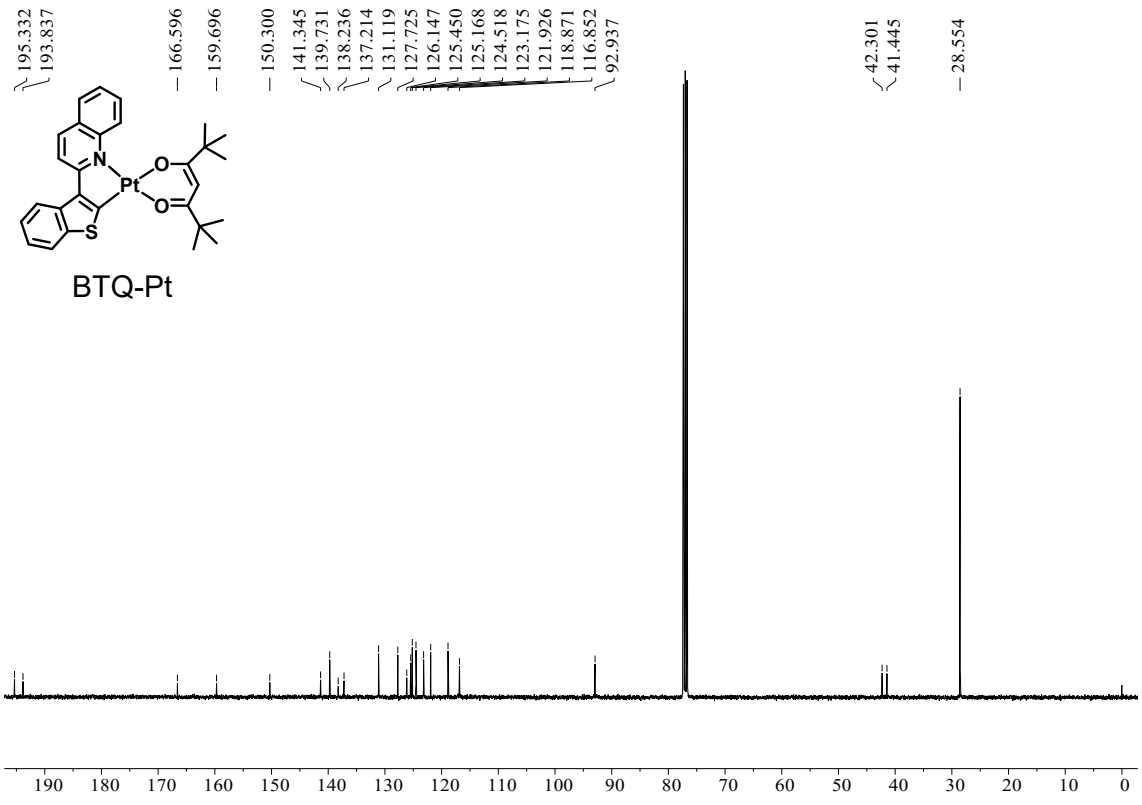
195.332
193.837
166.596
159.696
150.300
141.345
139.731
138.236
137.214
131.119
127.725
126.147
125.450
125.168
124.518
123.175
121.926
118.871
116.852
92.937
42.301
41.445
28.554
N
Pt
O
O
S
BTQ-Pt
190 180 170 160 150 140 130 120 110 100 90 80 70 60 50 40 30 20 10 0

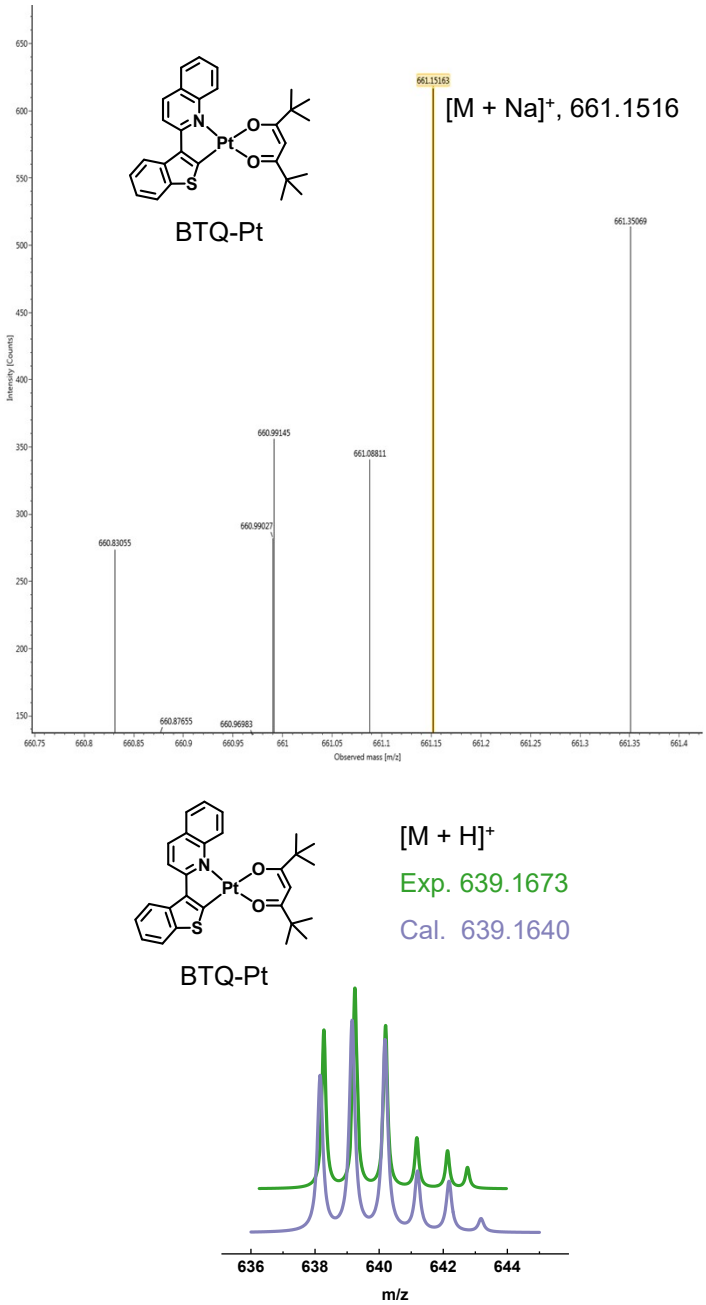

Figure S4. The ^{1}H, ^{13}C, HRMS and the measured (green trace) and simulated (purple trace) isotopic patterns of **BTQ-Pt**.

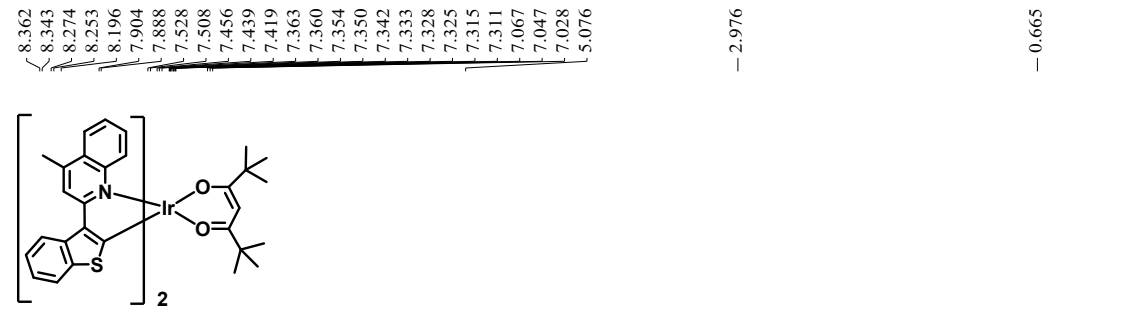

MBTQ-Ir

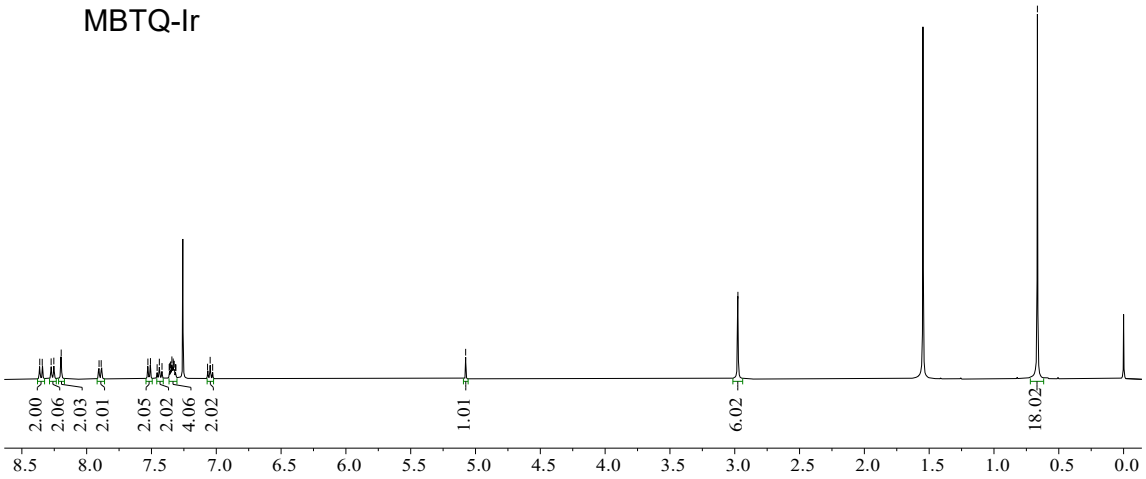

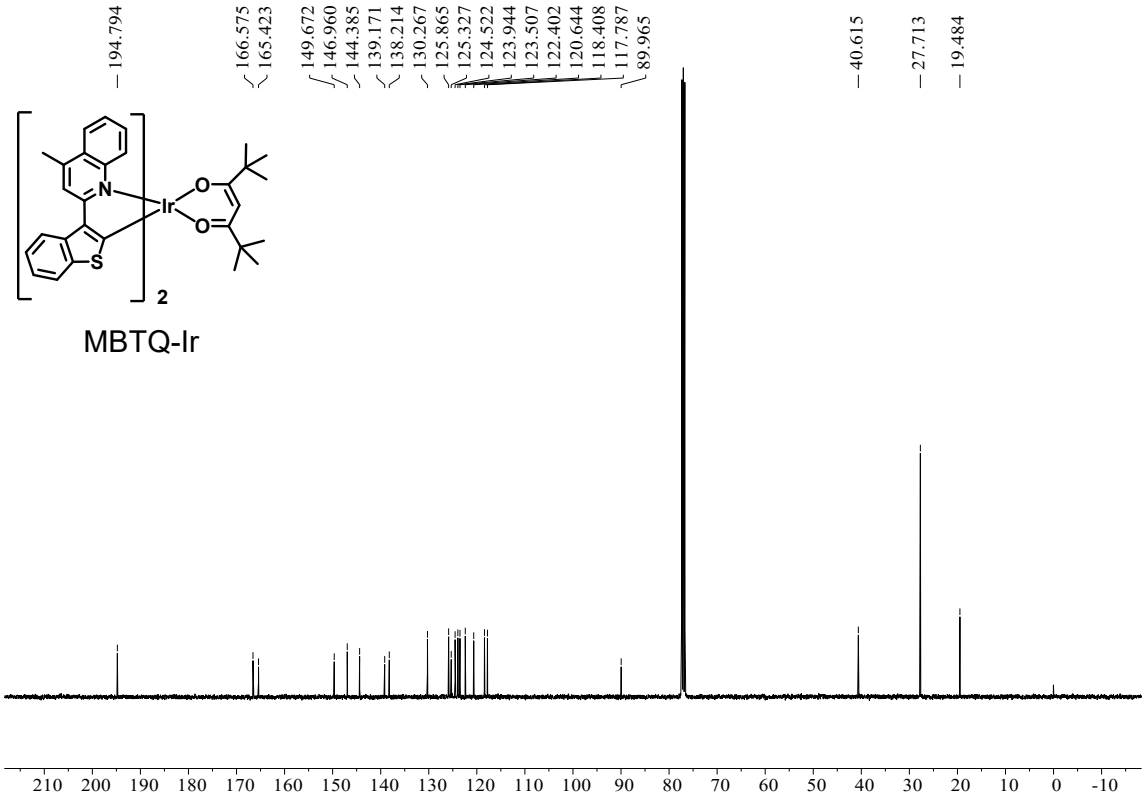

MBTQ-Ir

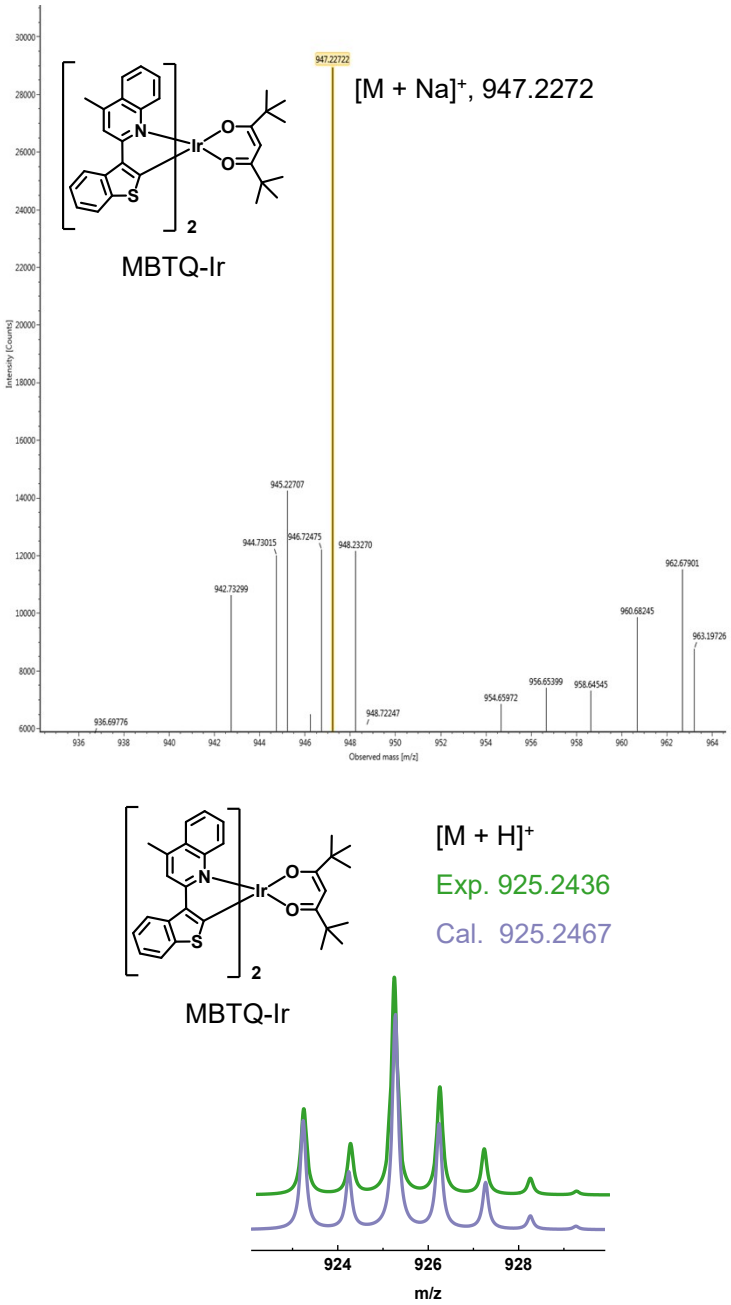

Figure S5. The ^{1}H, ^{13}C, HRMS and the measured (green trace) and simulated (purple trace) isotopic patterns of **MBTQ-Ir**.

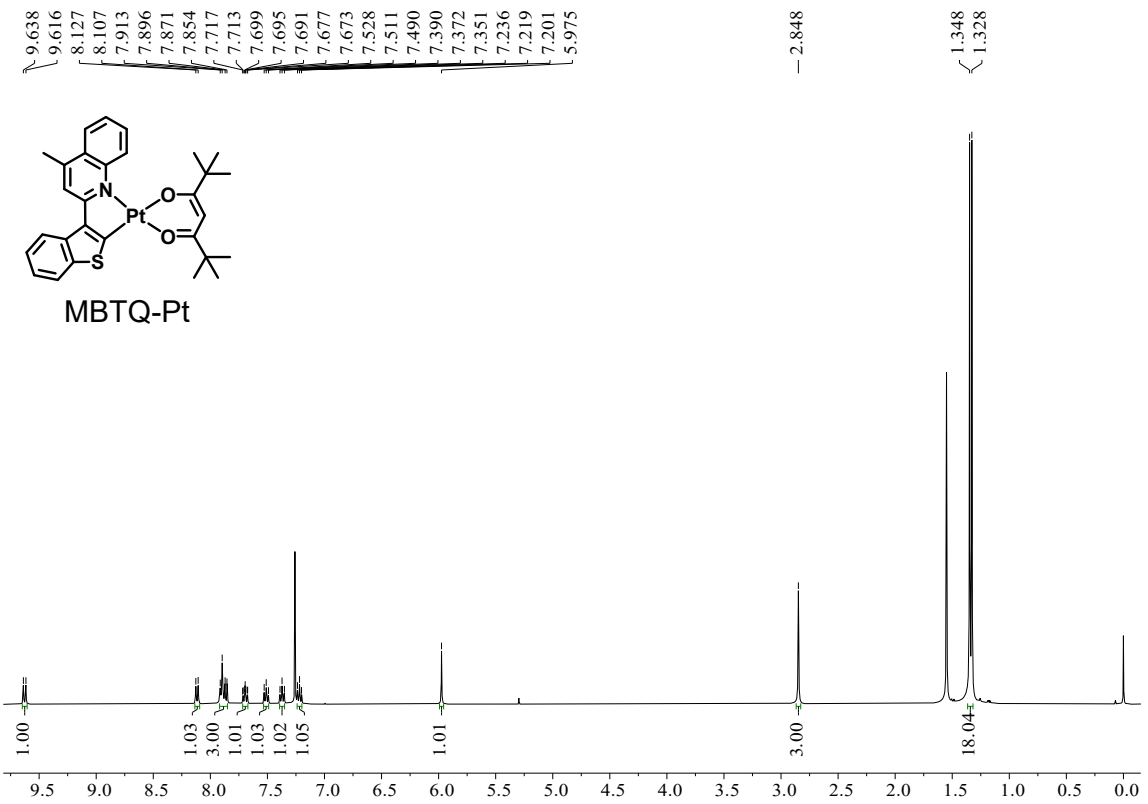
9.638
9.616
8.127
8.107
7.913
7.896
7.871
7.854
7.717
7.713
7.699
7.695
7.691
7.677
7.673
7.528
7.511
7.490
7.390
7.372
7.351
7.236
7.219
7.201
5.975
2.848
1.348
1.328
N
Pt
O
O
S
MBTQ-Pt
1.00
1.03
3.00
1.01
1.03
1.02
1.05
1.01
3.00
18.04
9.5
9.0
8.5
8.0
7.5
7.0
6.5
6.0
5.5
5.0
4.5
4.0
3.5
3.0
2.5
2.0
1.5
1.0
0.5
0.0

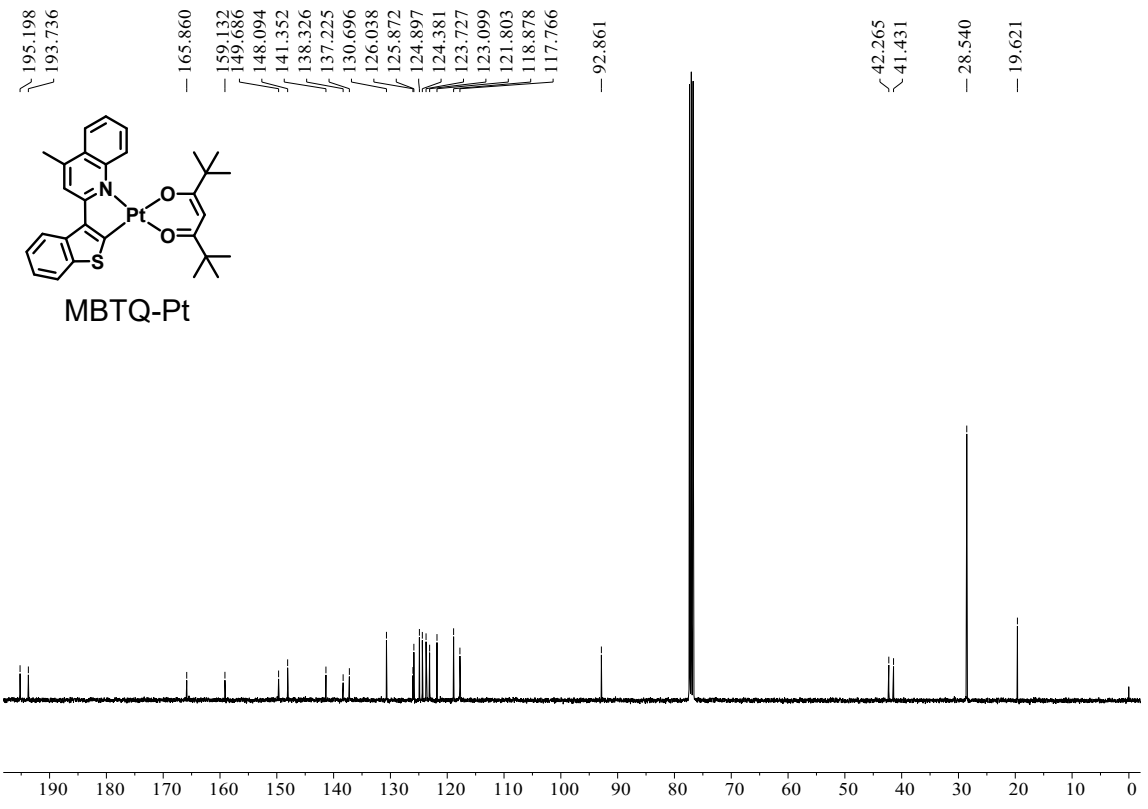
195.198
193.736
165.860
159.132
149.686
148.094
141.352
138.326
137.225
130.696
126.038
125.872
124.897
124.381
123.727
123.099
121.803
118.878
117.766
92.861
42.265
41.431
28.540
19.621
N
Pt
O
O
S
MBTQ-Pt
190
180
170
160
150
140
130
120
110
100
90
80
70
60
50
40
30
20
10
0

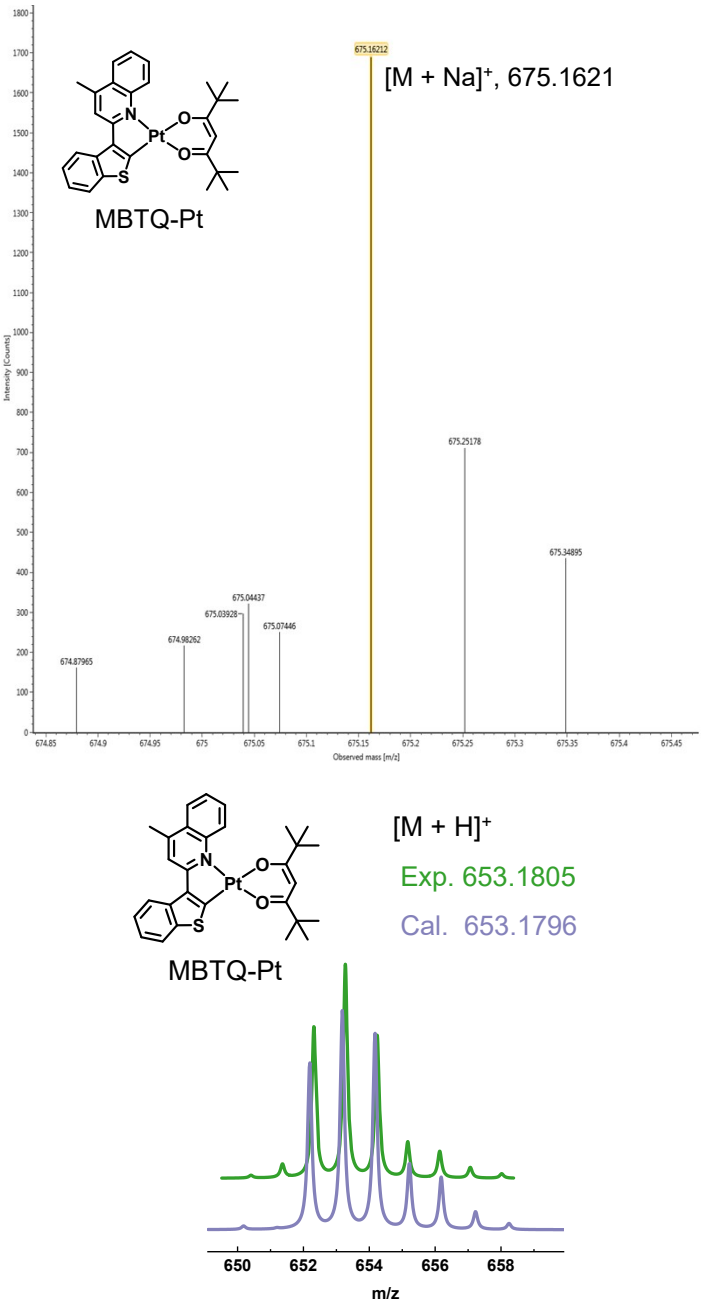

Figure S6. The ^{1}H, ^{13}C, HRMS and the measured (green trace) and simulated (purple trace) isotopic patterns of **MBTQ-Pt**.

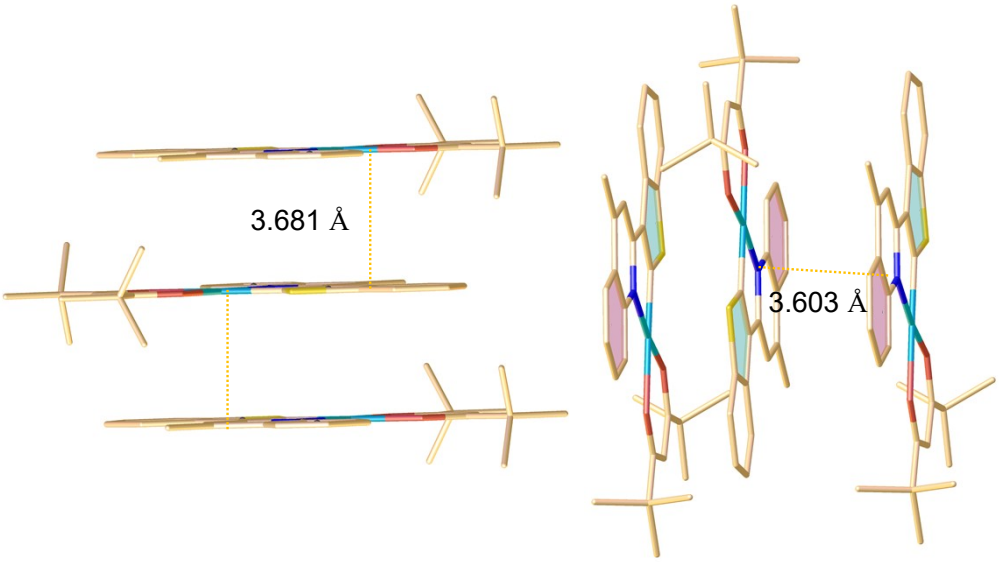

Figure S7. The π–π stacking interactions of MBTQ-Pt in crystal. Hydrogen atoms are omitted for clarity.

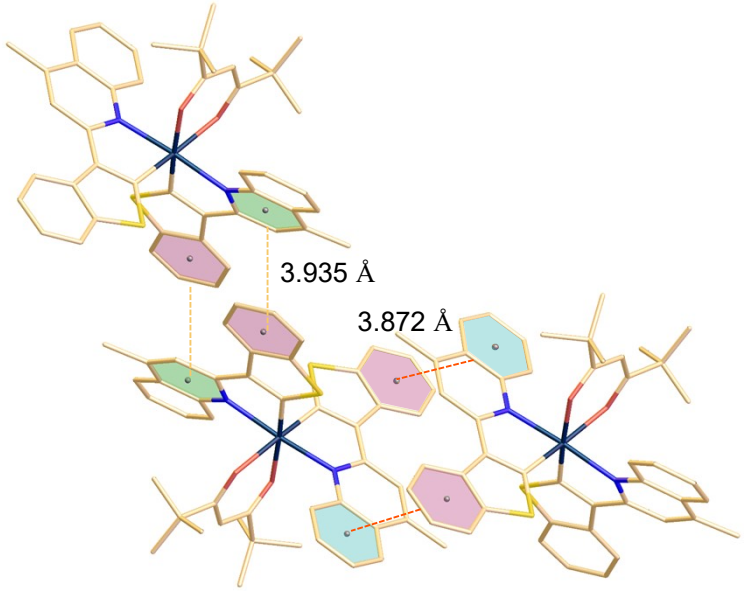

Figure S8. The π–π stacking interactions of MBTQ-Ir in crystal. Hydrogen atoms are omitted for clarity.

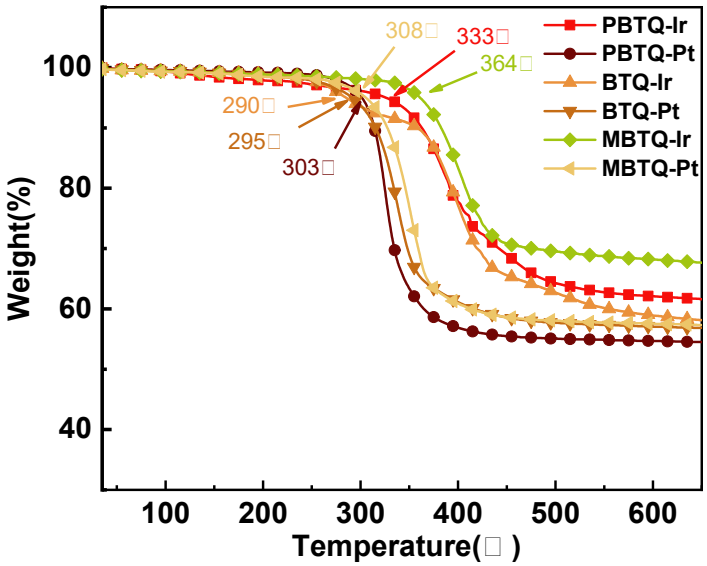

Figure S9. TGA curves of Pt(II) and Ir(III) complexes.

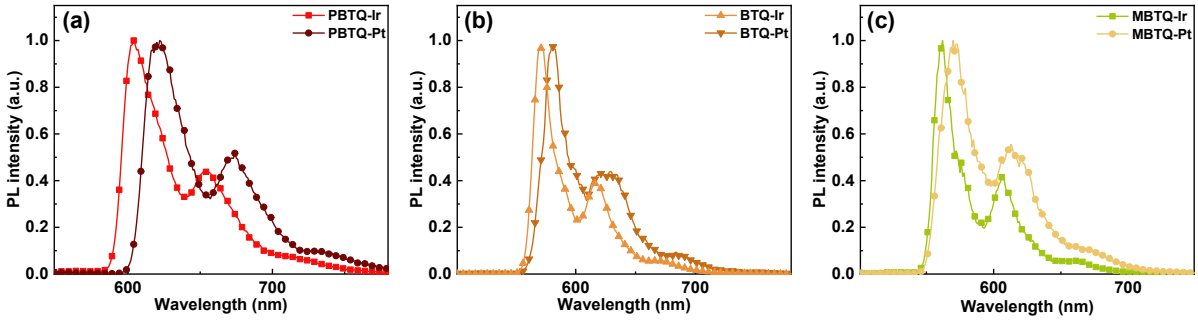

Figure S10. photoluminescence spectra of Ir(III) and Pt(II) complexes in the 2-MeTHFsolution (a) (b) (c) at 77K.

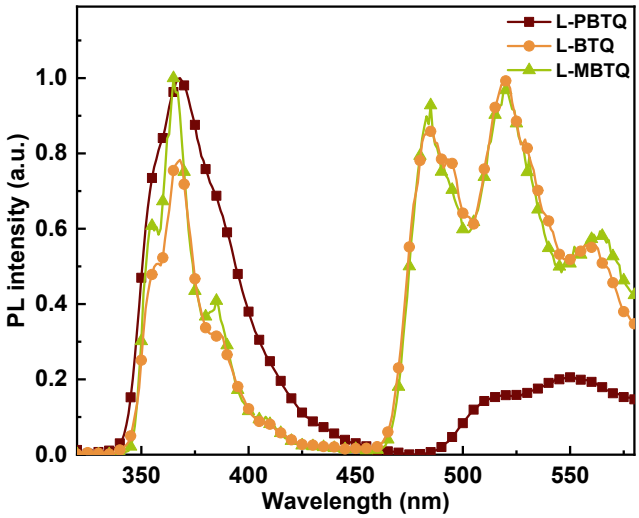

Figure S11. photoluminescence spectra of three ligands in the 2-MeTHFsolution at 77K.

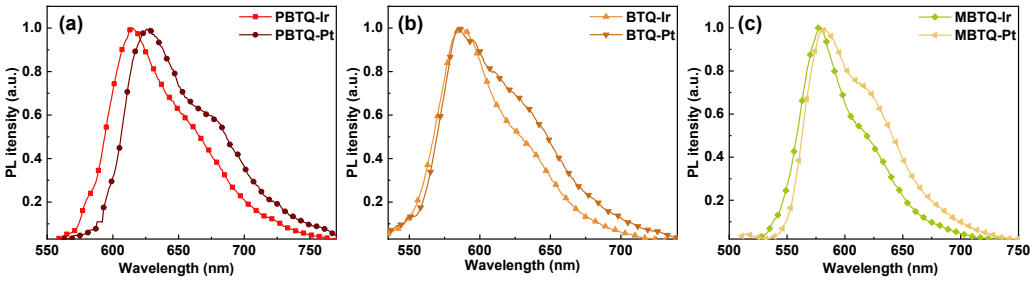

Figure S12. Photoluminescence spectra of Ir(III) and Pt(II) complexes in the doped PMMA films.

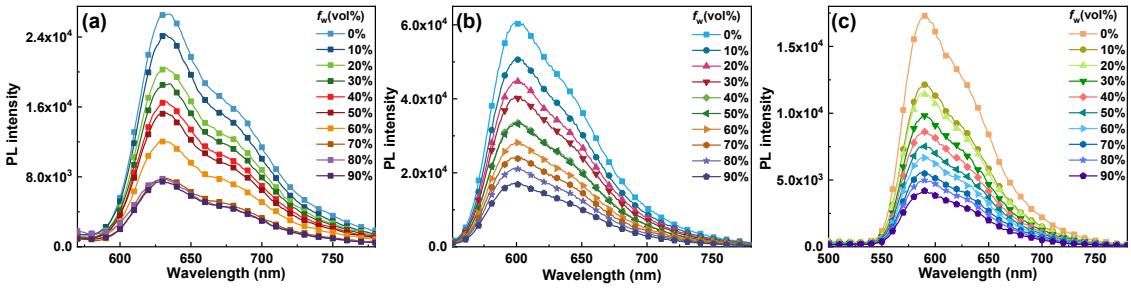

Figure S13. PL spectra of these Pt(II) complexes in DCM-MeOH mixture at different methanol fractions f_w under the same measurement conditions. (a) PBTQ-Pt, (b) BTQ-Pt1, (c) MBTQ-Pt.

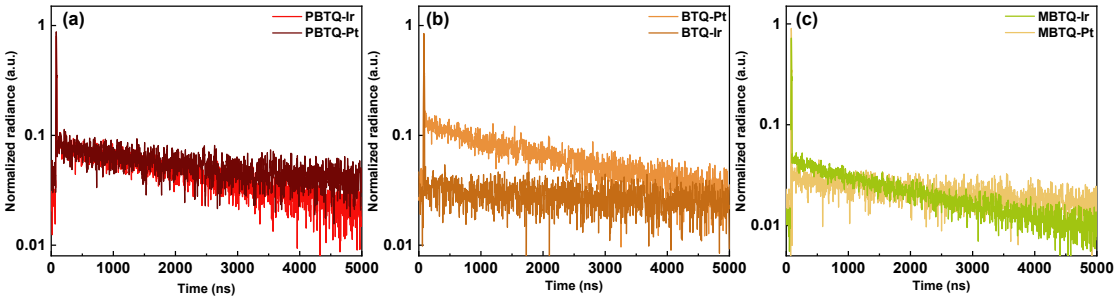

Figure S14. Transient decay in PMMA films (The doping concentrations of Pt(II) complexes and Ir(III) complexes are 2% and 4%, respectively.).

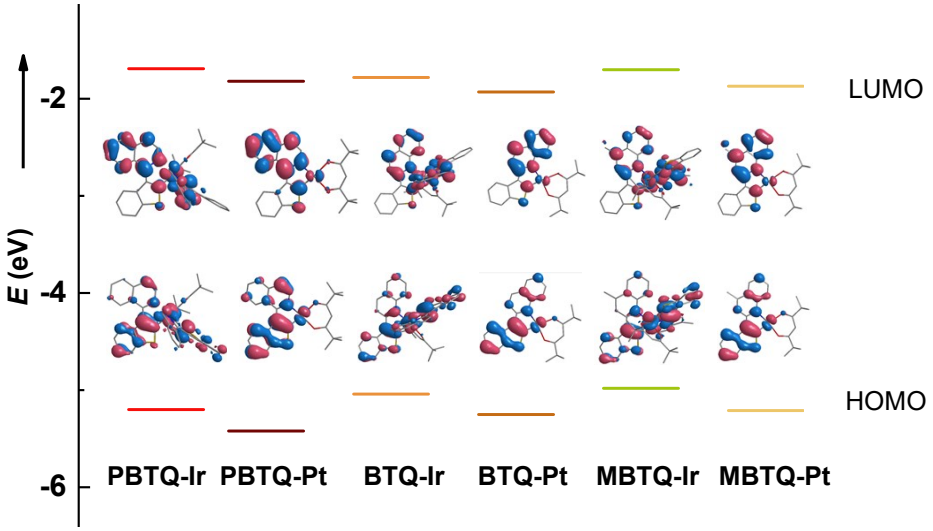

Figure S15. Molecular orbital (MO) distribution patterns of Ir(III) and Pt(II) complexes based on their optimized S_0 geometries.

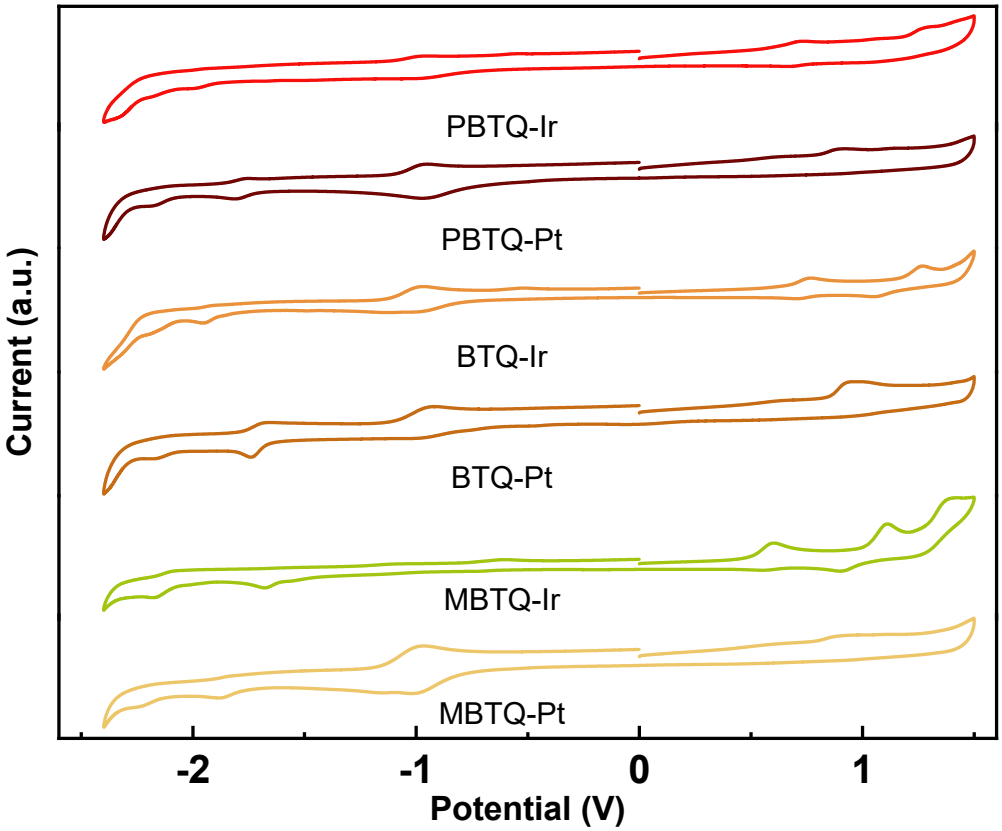

Figure S16. CV curves of these complexes.

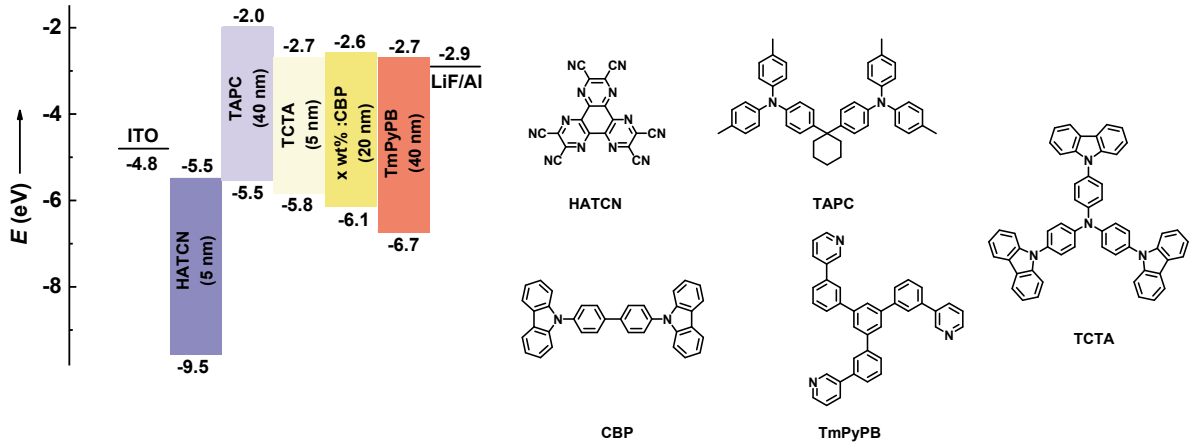

Figure S17. Energy levels and the chemical structures of materials used in OLEDs.

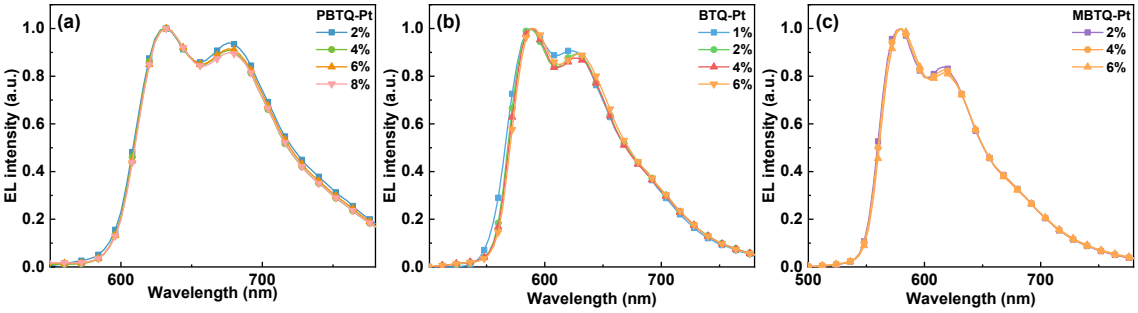

Figure S18. EL spectra at different CBP doping concentrations. (a) PBTQ-Pt, (b) BTQ-Pt, (c) MBTQ-Pt.

Table S1. Crystal data and structure refinement for **MBTQ-Ir**

Crystal data and structure refinement			
formula	$C_{47}H_{43}IrN_2O_2S_2$	ρ_{calc}(g cm^{-3})	1.532
M (g mol^{-})	924.24	μ(mm^{-1})	3.264
Crystal system	monoclinic	F(000)	4091.0
Space group	$P2_1/c$	2θ range for data collection/°	3.91 to 51.02
a/Å	19.5136(7)	Reflections collected	122150
b/Å	30.4253(11)	Independent reflections	16412
c/Å	15.9205(6)	R (I > 2σ(I))	R_1 = 0.0496, wR_2= 0.1084
α/°	90	R (all data)	R1 = 0.0589 wR_2 = 0.1131
β/°	111.0370(10)	Goodness-of-fit on F^2	1.108
γ/°	90		
Volume/Å^3	8822.1(6)		
Z	8		

Table S2. Selected bond lengths [Å] and angles [°] for MBTQ-Ir

Bond angles (°)		Bond lengths (Å)	
N1-Ir1-O2	80.67(18)	Ir1-N1	2.097(5)
N1-Ir1-O3	101.2(2)	Ir1-O2	2.123(4)
O3-Ir1-O2	86.64(17)	Ir1-O3	2.120(4)
N2-Ir1-N1	176.1(2)	Ir1-N2	2.093(5)
N2-Ir1-O2	101.86(18)	Ir1-C11	1.961(7)
N2-Ir1-O3	81.95(19)	Ir1-C27	1.969(6)
C11-Ir1-N1	78.4(2)		
C11-Ir1-O2	88.3(2)		
C11-Ir1-O3	174.9(2)		
C11-Ir1-N2	98.7(2)		
C11-Ir1-C27	97.6(3)		
C27-Ir1-N1	99.2(2)		
C27-Ir1-O2	173.9(2)		
C27-Ir1-O3	87.4(2)		
C27-Ir1-N2	78.6(2)		

Table S3. Crystal data and structure refinement for **MBTQ-Pt**

Crystal data and structure refinement			
formula	$C_{29}H_{31}NO_2PtS$	ρ_{calc}(g cm^{-3})	1.745
M (g mol^{-})	652.70	μ(mm^{-1})	5.760
Crystal system	monoclinic	F(000)	644.0
Space group	$P2_1/m$	2θ range for data collection/°	5.454 to 55.042
a/Å	14.0035(6)	Reflections collected	43568
b/Å	6.9360(4)	Independent reflections	3072
c/Å	14.2412(10)	R (I > 2σ(I))	R_1 = 0.0151 wR_2= 0.0369
α/°	90	R (all data)	R1 = 0.0152, wR_2 = 0.0370
β/°	116.126(2)	Goodness-of-fit on F^2	1.121
γ/°	90		
Volume/Å^3	1241.90(14)		
Z	2		

Table S4. Selected bond lengths [Å] and angles [°] for MBTQ-Pt

Bond angles (°)		Bond lengths (Å)	
O1-Pt1-O2	87.35(7)	Pt1-N1	2.063(2)
O1-Pt1-N1	168.56(8)	Pt1-C21	1.923(3)
N1-Pt-O2	104.09(8)	Pt1-O2	2.088(18)
C21-Pt-O1	89.47(9)	Pt1-O1	1.992(18)
C21-Pt-O2	176.81(8)		
C21-Pt-N1	79.10(9)		

Table S5. Theoretical calculation results for complexes based on their optimized S_0 geometries.

Complex	MO	Contribution percentages of metal d_π orbitals and π orbitals of ligand to MOs (%)			Main configuration of $S_0 \rightarrow S_1$ excitation/λ_{cal} (nm) [a]	Main configuration of $S_0 \rightarrow T_1$ excitation/ λ_{cal} (nm)[a]
MBTQ-Ir	Ir	L-MBTQ	L-tmd		H→L (90.10%)	H→L (46.27%)
	L+1	7.11	91.50	1.39	/456.67	/604.44
	L	4.15	93.78	2.07		
	H	17.18	83.59	2.23		
	H-1	19.94	75.92	4.14		
MBTQ-Pt	Pt	L-MBTQ	L-tmd		H→L (96.10%)	H→L (84.69%)
	L+1	1.11	42.71	56.18	/442.76	/612.97
	L	7.36	90.94	1.67		
	H	16.99	80.60	2.41		
	H-1	23.41	34.57	42.05		
BTQ-Ir	Ir	L-BTQ	L-tmd		H→L (97.59%)	H→L (70.67%)
	L+1	3.70	95.54	0.76	/466.65	573.02
	L	5.01	92.96	2.03		
	H	19.74	78.76	1.50		
	H-1	15.43	83.22	1.35		
BTQ-Pt	Pt	L-BTQ	L-tmd		H→L (96.63%)	H→L (88.47%)
	L+1	1.76	10.40	87.84	450.18	575.93

	L	6.54	92.34	1.12		
	H	17.69	79.60	2.71		
	H-1	23.33	33.19	43.48		
MBTQ-Ir	Ir		L-MBTQ	L-tmd	H→L (97.69%)	H→L (71.31%)
	L+1	3.54	95.92	0.54	463.43	568.42
	L	4.71	93.33	1.96		
	H	20.09	78.47	1.44		
	H-1	16.00	82.60	1.40		
MBTQ-Pt	Pt		L-MBTQ	L-tmd	H→L (93.75%)	H→L (87.65%)
	L+1	1.79	8.84	89.37	376.37	570.15
	L	6.18	92.74	1.08		
	H	17.73	79.60	2.67		
	H-1	24.41	32.29	43.30		

[a] H and L stand for HOMO and LUMO, respectively. L-PBTQ, L- BTQ, L- MBTQ and L-tmd are corresponding organic ligands. λ_{cal} denote calculated absorption wavelength

Table S6. NTO results for complexes based on optimized T_1 geometries.

complex	NTO [a]	Contribution percentages of metal d_π orbitals and π orbitals of ligand to NTOs (%)		
		Ir	L-PBTQ	L-tmd
PBTQ-Ir	P	5.90	85.21	8.89
	H	21.37	55.69	22.94
		Pt	L-PBTQ	L-tmd
PBTQ-Pt	P	8.25	90.27	1.48
	H	11.29	87.91	0.80
		Ir	L-BTQ	L-tmd
BTQ-Ir	P	6.07	91.58	2.35
	H	25.01	73.46	1.53
		Pt	L-BTQ	L-tmd
BTQ-Pt	P	8.86	89.52	1.62
	H	15.56	83.28	1.16
		Ir	L-BTQ	L-tmd
MBTQ-Ir	P	5.75	91.97	2.28
	H	25.20	73.36	1.44
		Pt	L-BTQ	L-tmd
MBTQ-Pt	P	8.49	89.96	1.55
	H	15.44	83.37	1.19

Table S7. Summary of EL performance of Ir(III) complexes employing thiophene and benzothiophene OLEDs.

	λ_{EL} (nm)	EQE (%)	Reference
Ir(III) complex	576	20.3	This work
Ir(III) complex	575	17.9	Dyes Pigments., **2019**, 162 863-871
Ir(III) complex	654	10.8	Dyes Pigments., **2019**, 162 863-871
Ir(III) complex	620	10.4	ACS Appl. Mater. Interfaces., **2019**, 11, 26152−26164
Ir(III) complex	627	10.2	Dyes Pigments., **2025,** 235 112620
Ir(III) complex	623	15.42	Dyes Pigments., **2017**, 139, 779-787
Ir(III) complex	610	14.94	Mol. Cryst. Liq. Cryst., **2017**, 659, 108-114
Ir(III) complex	577	15.3	Dyes Pigments., **2025** 235, 112620
Ir(III) complex	627	10.2	Dyes Pigments., **2025**, 235, 112620
Ir(III) complex	556	18.2	Dalton Trans., **2020**, 49, 13797–13804
Ir(III) complex	562	10.9	Dalton Trans., **2020**, 49, 13797–13804
Ir(III) complex	628	8.2	Org. Electron., **2015**, 21, 1–8
Ir(III) complex	588	11.2	Org. Electron., **2013,** 14, 3392–3398

REFERENCES

[1] G.M. Sheldrick, Acta. Crystallogr. C Struct. Chem. 71 (2015) 3-8.

[2] O.V. Dolomanov, L.J. Bourhis, R.J. Gildea, et al., J. Appl. Crystallogr. 42 (2009) 339-341.

[3] G.M. Sheldrick, Acta. Crystallogr. A Found. Adv. 71 (2015) 3-8.

[4] W.R. Wadt, P.J. Hay, J. Chem. Phys. 82 (1985) 284-298.

[5] P.J. Hay, W.R. Wadt, J. Chem. Phys. 82 (1985) 299-310.

[6] M.J. Frisch, G.W. Trucks, H.B. Schlegel, et al., Gaussian 16 Rev. B.01, Wallingford, CT, 2016.